# Polycomb group RING finger proteins 3/5 activate transcription via an interaction with the pluripotency factor Tex10 in embryonic stem cells

Received for publication, June 23, 2017, and in revised form, October 11, 2017 Published, Papers in Press, October 20, 2017, DOI 10.1074/jbc.M117.804054

**Wukui Zhao[‡], Yikai Huang[‡], Jingzi Zhang[‡], Mengjie Liu[‡], Haijing Ji[§], Congcong Wang[‡], Ning Cao[‡], Chaojun Li[‡], Yin Xia[¶], Qing Jiang[‖], and Jinzhong Qin[‡1]**

*From the [‡]MOE Key Laboratory of Model Animal for Disease Study, Model Animal Research Center, Nanjing Biomedical Research Institute, Nanjing University, 12 Xuefu Road, Nanjing, Jiangsu 210061, the [§]College of Animal Science and Technology, Nanjing Agricultural University, Nanjing 210014, the [¶]School of Biomedical Sciences, Chinese University of Hong Kong, Hong Kong, and the [‖]Department of Sports Medicine and Adult Reconstructive Surgery, Nanjing Drum Tower Hospital, Medical School of Nanjing University, Nanjing 21008, China*

Edited by Ronald C. Wek

**Polycomb group (PcG) proteins are epigenetic transcriptional repressors that orchestrate numerous developmental processes and have been implicated in the maintenance of embryonic stem (ES) cell state. More recent evidence suggests that a subset of PcG proteins engages in transcriptional activation in some cellular contexts, but how this property is exerted remains largely unknown. Here, we generated ES cells with single or combined disruption of polycomb group RING finger protein 3 (Pcgf3) and Pcgf5 with the CRISPR-Cas9 technique. We report that although these mutant cells maintained their self-renewal and colony-forming capacity, they displayed severe defects in mesoderm differentiation *in vitro* and *in vivo*. Using RNA-seq to analyze transcriptional profiles of ES cells with single or combined Pcgf3/5 deficiencies, we found that in contrast to the canonical role of the related polycomb repressive complex 1 (PRC1) in gene repression, Pcgf3/5 mainly function as transcriptional activators driving expression of many genes involved in mesoderm differentiation. Proteomic approaches and promoter occupancy analyses helped to establish an extended Pcgf3/5 interactome and identified several novel Pcgf3/5 interactors. These included testis-expressed 10 (Tex10), which may directly contribute to transcriptional activation via the transcriptional co-activator p300. Furthermore, Pcgf3/5 deletion in ES cells substantially reduced the occupancy of Tex10 and p300 at target genes. Finally, we demonstrated that Pcgf3/5 are essential for regulating global levels of the histone modifier H2AK119ub1 in ES cells. Our findings establish Pcgf3/5 as transcriptional activators that interact with Tex10 and p300 in ES cells and point to redundant activity of Pcgf3/5 in pluripotency maintenance.**

Embryonic stem (ES)[2] cells are characterized by their capacity to self-renew and to differentiate into almost all cell lineages of the body and provide a valuable tool for studying developmental processes *in vitro* (1, 2). A large body of evidence suggests that PcG proteins are the essential epigenetic regulators involved in ES cell pluripotency and differentiation (3, 4). The PcG was originally described as a set of genes responsible for controlling proper body segmentation in *Drosophila* (5), by maintaining a transcriptionally repressed state of Hox gene expression (6). In mammals, PcG proteins mediate developmental gene silencing via the formation of at least two distinct protein complexes known as PRC1 and PRC2 (7, 8). PRC2 consists of the core subunits Eed, Suz12, and Ezh1/2 and di- and trimethylates histone H3 at lysine 27 (H3K27me2/3) (9). PRC1 contains the E3 ligases Ring1A/B, which monoubiquitinate lysine 119 at histone H2A (H2AK119ub1) (10). PRC1 can be distinguished based on their subcomponent composition as canonical and non-canonical PRC1. According to this classification, canonical PRC1s contain Cbx proteins (Cbx2/4/6/7/8), Phc1/2/3, Pcgf2/4, and Ring1A/B. By contrast, non-canonical PRC1s contain Rybp or Yaf2 instead of Cbxs (11). Further diversification of PRC1 emerges from the mutually exclusive association of Ring1A/B with Pcgf1–6. There are at least six different groups of PRC1 complexes, PRC1.1–1.6, each comprising one of six Pcgf (12).

Pcgf3 and Pcgf5 have been characterized as a key component of non-canonical PRC1.3 and PRC1.5, respectively, both of which share Ring1A/B, Rybp/Yaf2, casein kinase 2 (Ck2), and Auts2 (autism susceptibility candidate 2) observed in 293T-REx cells (12). Recently, increasing evidence suggests that some PcG complexes act as transcriptional activators, indicating that the initial classification of PcG proteins as transcriptional repressors may not be generally applicable (13–15). However, the underlying mechanism of PcG-mediated gene activation

This work was supported by National Natural Science Foundation of China Grants 31471387 and 31671532 and the 2015 Shuangchuang Program of Jiangsu Province (to J. Q.). This project was supported by Nanjing University Innovation and Creative Program for Ph.D. Candidates Grant 2016027 (to W. Z.). The authors declare that they have no conflicts of interest with the contents of this article.

This article contains Tables S1–S3 and Figs. S1–S8.

*The microarray data have been deposited to the GEO database and are available under accession ID GSE102774.*

[1] To whom correspondence should be addressed. Tel.: 86-025-58641504; Fax: 86-025-58641500; E-mail: qinjz@nicemice.cn.

[2] The abbreviations used are: ES, embryonic stem; EB, embryoid body; PRC1, polycomb-repressive complex 1; PRC2, polycomb-repressive complex 2; sgRNA, single guide RNA; PcG, polycomb group; Ck2, casein kinase 2; LIF, leukemia inhibitory factor; qPCR, quantitative PCR; SMA, smooth muscle actin; GO, gene ontology; 5FMC, five friends of methylated Chtop; H2AK and H3K, histone 2A and 3 lysine, respectively.



© 2017 by The American Society for Biochemistry and Molecular Biology, Inc. Published in the U.S.A.

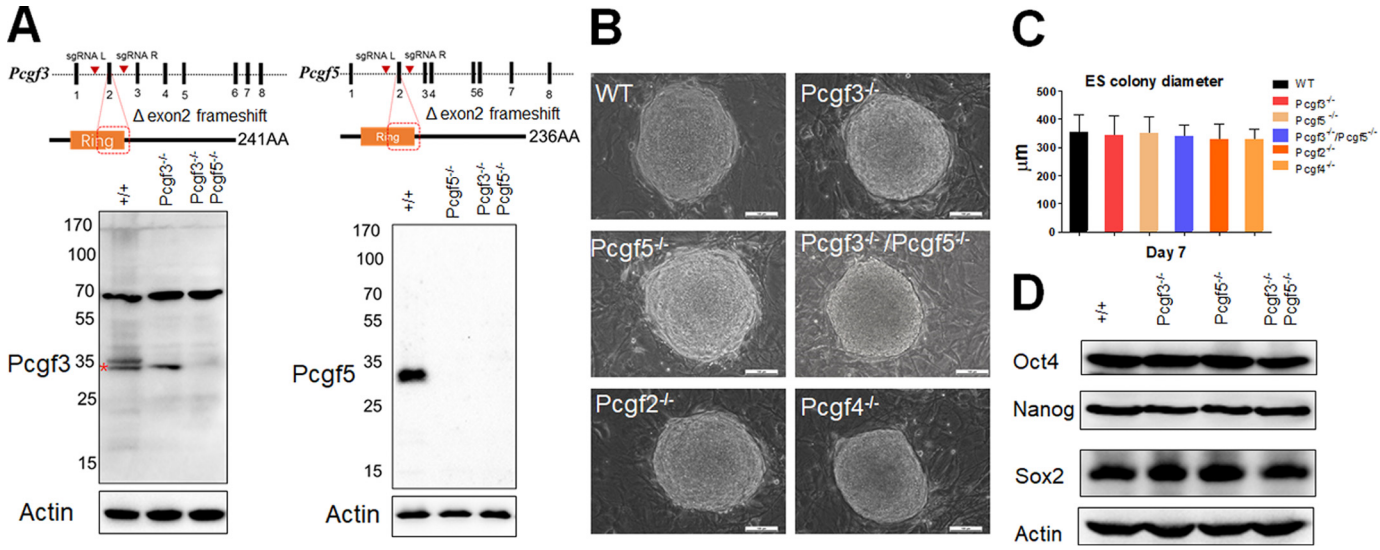


**Figure 1. Pcgf3/5 are dispensable for ES cell self-renewal.** *A*, schematic of the experimental strategy to knock out Pcgf3/5 in mouse ES cells via CRISPR/Cas9-assisted gene targeting. Western blot analysis (*below*) was used to demonstrate the loss of Pcgf3 or Pcgf5 expression in Pcgf3$^{-/-}$ or Pcgf5$^{-/-}$ mouse ES cells, respectively. Notably, the Pcgf3 antibody could nonspecifically bind Pcgf5 (*) in wild-type and Pcgf3$^{-/-}$ ES cells but not in Pcgf3$^{-/-}$/Pcgf5$^{-/-}$ ES cells. *B*, representative phase-contrast images of ES cell colonies of the indicated genotypes. All ES cell colonies were photographed at day 7 after seeding single-cell suspensions on feeder layers. *C*, bar graphs show the mean diameter of 20 random ES cell colonies. Images were taken at ×200 magnification at day 7. Data represent the average of three independent experiments. *D*, protein levels of pluripotency markers were determined by Western blotting in ES cells of the indicated genotypes. Notably, four independently derived ES cell clones deficient in Pcgf3/5 either alone or together had been analyzed with similar results in each of the assays described in this figure.

remains largely unknown. Of note, Auts2, a component of PRC1.5, has recently been shown to render this complex capable of activating transcription through its recruitment of Ck2 and interaction with p300 in developing neuronal cells (16). Although recent studies implicate L(3)73Ah, a homolog of mammalian Pcgf3, in regulating global H2AK118ub1 level in *Drosophila*, by forming a dimer with Ring1 (17), the function of Pcgf3 and Pcgf5 in mammals remains to be determined.

Here, we generated ES cells with single or combined disruption of Pcgf3/5 via CRISPR/Cas9-mediated genetic engineering. We showed that although Pcgf3 or Pcgf5 mutant cells are viable and retain their typical undifferentiated ES cell morphology, loss of Pcgf3 or Pcgf5 impairs proper differentiation of ES cells into mesoderm *in vitro* and *in vivo*. Additionally, Pcgf3/5 protein complexes in ES cells are purified using a biochemical-based affinity purification and subsequently analyzed by means of MS. We find that Pcgf3/5 can form novel non-canonical PRC1 complexes that contain Ck2s (Ck2a1, Ck2a2, and Ck2b) and Tex10 in ES cells. Finally, we show that p300 is recruited to Pcgf3/5 target genes through its interaction with Tex10 and might contribute to transcriptional activation.

## Results

### *Pcgf3/5 are not essential for ES cell self-renewal*

To explore the function of Pcgf3 and Pcgf5 in the maintenance of ES cells, we first generated Pcgf3 or Pcgf5 knockout ES cell lines using the CRISPR/Cas9 technique (18). To delete the region encoding the RING finger motif and introduce a frameshift, we designed two single guide RNAs (sgRNAs) specifically flanking exon 2 of the mouse *Pcgf3* or *Pcgf5* gene. Independent ES cell clones were isolated, and genomic deletions were confirmed by PCR with primers outside the expected cleavage site (19) (Fig. S1). Western blot analysis revealed complete loss of Pcgf3 or Pcgf5 proteins in targeted deletion mutant ES cells, and no truncated proteins were detected (Fig. 1*A*). Pcgf3 and Pcgf5 share 57.9% amino acid homology and are found in complexes with similar subunit composition (see below). To test for possible functional redundancy between Pcgf3 and Pcgf5 in ES cells, we also generated ES cells with double knockout of the genes for Pcgf3 and Pcgf5.

ES cells with single or double knockout of Pcgf3/5 were viable and retained the normal ability to form a typical undifferentiated ES cell colony after being seeded on mitomycin-C-irradiated mouse embryonic fibroblasts. Furthermore, colony size of different mutants was comparable with that of wild type (Fig. 1, *B* and *C*). Immunoblotting of the pluripotent factors indicated that knockout of Pcgf3, Pcgf5, or both in ES cells did not significantly alter the protein levels of the core pluripotency markers Oct4, Nanog, and Sox2 (Fig. 1*D*), consistent with the undifferentiated morphology observed in these mutants. Notably, an identical phenotype was obtained from each of the four independently derived clones of ES cells deficient in Pcgf3/5 either alone or together (Fig. S1). In addition, a very similar phenotype was observed in Pcgf2 (Mel18) or Pcgf4 (Bmi1), core components of canonical PRC1 complexes PRC1.2 and PRC1.4, respectively, knockout ES cells (Fig. 1*B* and Figs. S2 and S3). These observations, together with our previous findings (19, 20), strongly suggest that all PCGF family members except for Pcgf6 are dispensable for the self-renewal of ES cells.

### *Pcgf3/5 are necessary for mesoderm differentiation*

Embryoid bodies (EBs) mimic early development of the embryo and are often used as an *in vitro* differentiation assay to test ES cell pluripotency (21). Our previous study revealed that loss of Pcgf1 severely impairs ES cell differentiation *in vitro*, mainly due to a failure to initiate the proper differentiation

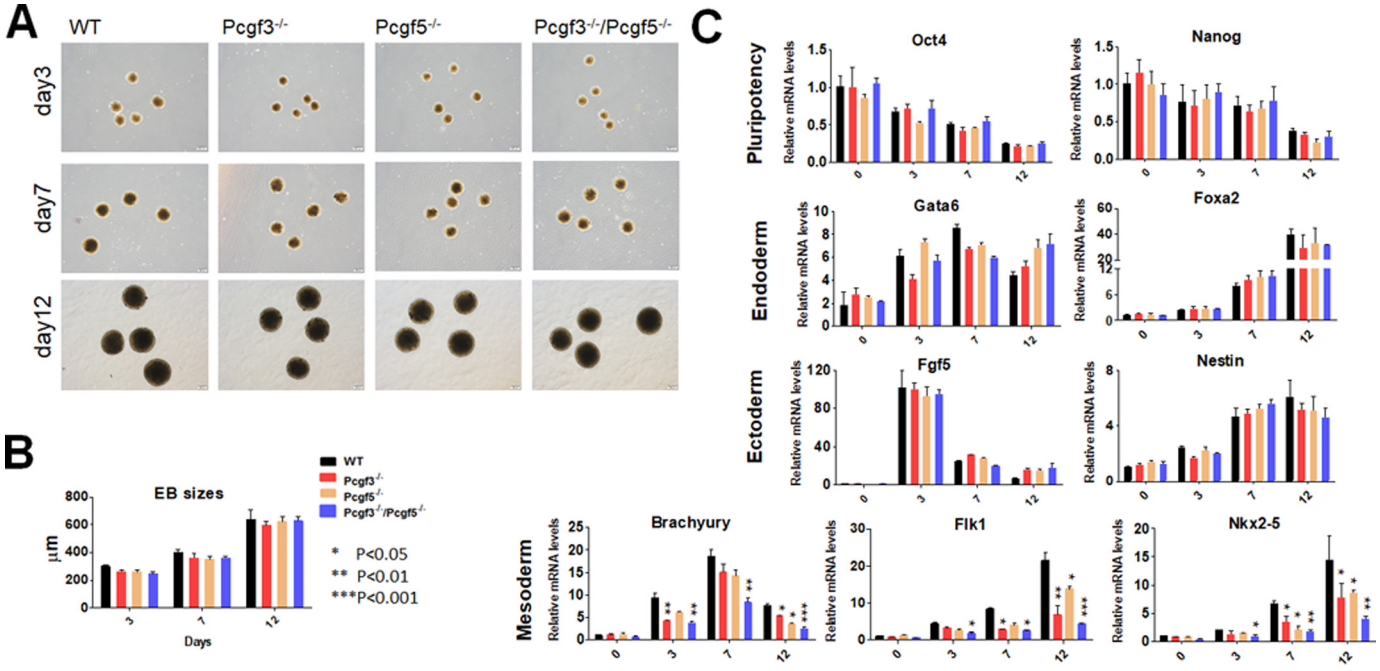


**Figure 2. Pcgf3/5 null ES cells display defective mesoderm differentiation *in vitro*.** *A*, morphology and characterization of EBs of the indicated genotypes at days 3, 7, and 12 in suspension culture. Images were taken at ×40 magnification. *B*, bar graphs indicate the mean diameters of 20 random EBs of the indicated genotypes. Data represent the average of three independent experiments. *C*, RT-qPCR of selected genes in ES cells and differentiated EBs at days 3, 7, and 12. Of note, genes related to mesoderm differentiation (Brachyury, Flk1, and Nkx2-5) were strongly down-regulated in mutant EBs. Expression was normalized to the housekeeping gene β-actin. *Error bars*, S.D. Bar graphs represent the mean of three independent biological repeats. *p* values were from Student's *t* test analysis. Notably, four independently derived ES cell clones deficient in Pcgf3/5 either alone or together had been analyzed with similar results in each of the assays described in this figure.

program, and Pcgf6 mutant ES cells display skewed differentiation toward endoderm lineage in EBs (19, 20). Additionally, Pcgf2 has been described as being important for cardiac development and differentiation *in vitro* by knockdown of Pcgf2 in ES cells (22). To test whether Pcgf3 or Pcgf5 plays a role in ES cell differentiation, the mutant and wild-type ES cells were cultured without feeder cells and leukemia-inhibitory factor (LIF) to aggregate in hanging drops to form EBs. Specifically, wild-type, Pcgf3/5 single and double knockout ES cells were cultured in hanging drops for 3 days and subsequently maintained in rotating conditions without LIF, where cells differentiated into the three germ layers (ectoderm, mesoderm, and endoderm). EB morphology was examined by microscopy (Fig. 2*A*). As shown in Fig. 2*B*, the mutant ES cells retained their ability to form EBs of a size similar to those derived from control cells. Total RNA was isolated from ES cells and EBs at 3, 7, and 12 days of culture, followed by quantitative real-time RT-PCR (qPCR) analysis of core pluripotency gene transcript levels as well as markers of lineage-specific differentiation. Expression of the core pluripotency markers Oct4 and Nanog was efficiently down-regulated, whereas the lineage-specific differentiation markers, including endodermal (Gata6 and Foxa2), ectodermal (Fgf5 and Nestin), and mesodermal (Brachyury, Flk1, and Nkx2-5) markers, were up-regulated during the differentiation process, consistent with the onset of the differentiation program in both mutant and wild-type cells. Importantly, throughout mutant EB culture, all mutants showed markedly decreased expression levels of mesoderm markers with respect to control EBs, whereas no differences in the levels of endoderm and ectoderm markers were observed between mutants and wild type (Fig. 2*C*), indicating that Pcgf3/5 are necessary for proper mesodermal lineage differentiation during EB culture. Notably, Pcgf3/5 double knockout EBs displayed more pronounced decrease in the expression of mesoderm markers than any of the corresponding single mutants, suggesting that Pcgf3/5 have partially redundant functions during EB differentiation (Fig. 2*C*). We also checked the protein levels of those germ layer markers in differentiated EBs and found that protein levels of mesoderm markers, including Brachyury and Flk1, were dramatically decreased in differentiated EBs at day 12 with respect to control (Fig. S4). However, no differences in the protein levels of ectoderm marker Nestin were observed between mutants and wild type. Remarkably, lentiviral expression of FLAG-tagged Pcgf3/5 was able to rescue the protein levels of mesoderm markers to levels similar to those in control cells (Fig. S4), indicating that the observed differentiation phenotypes are caused by Pcgf3/5 deficiencies. Furthermore, to assess whether Pcgf3/5 knockout ES cells give rise to terminally differentiated cells, these cells were subcutaneously injected into immune-deficient mice. Immunohistochemistry of wild-type ES cell-derived teratomas with antibody specific to α-smooth muscle actin (SMA; mesoderm marker) revealed large numbers of SMA-positive cells, whereas teratomas derived from ES cells with Pcgf3/5 single or combined loss had marked decreases in SMA-positive cells. Notably, Pcgf3/5 ablation has no effect on endoderm and ectoderm specification, as evidenced by TROMA1 and GFAP staining, respectively (Fig. S5). Taken together, Pcgf3 and Pcgf5 have a redundant but essential role in ES cell mesoderm differentiation *in vitro* and *in vivo*.

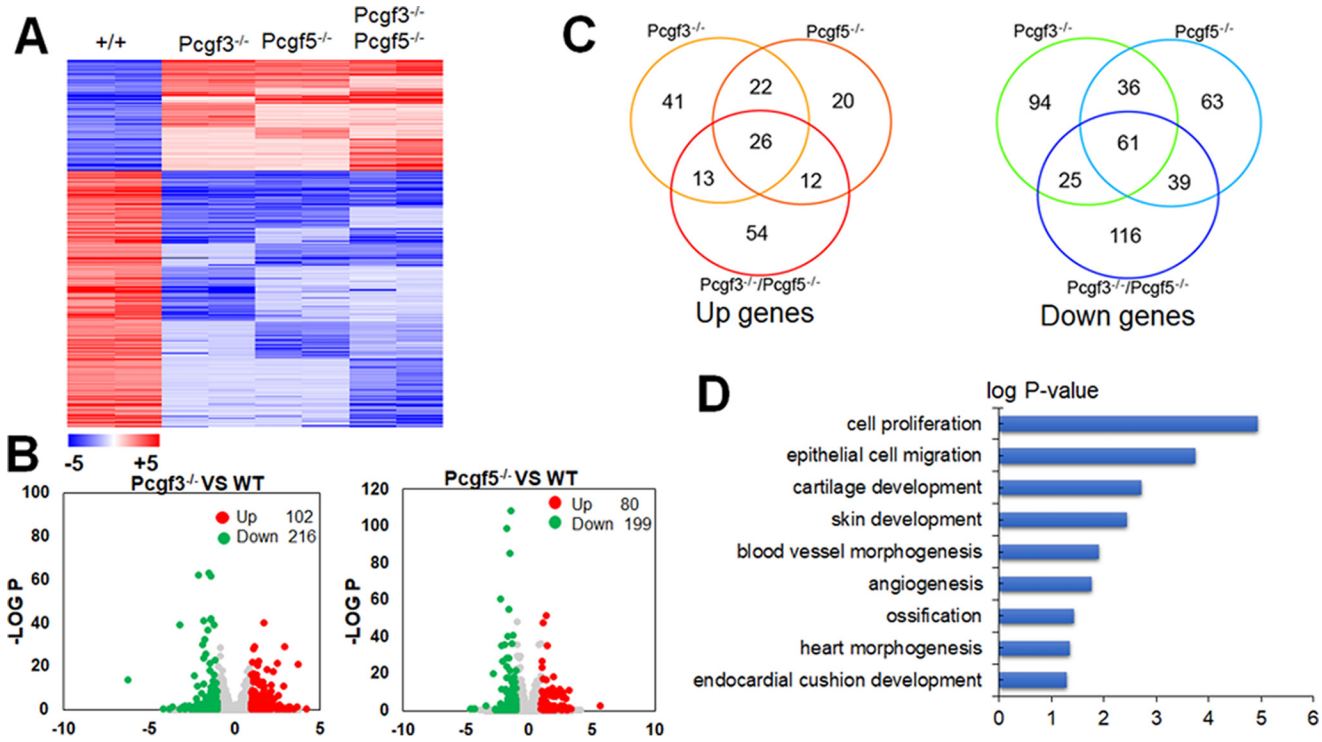


**Figure 3. Gene expression profiling in ES cells lacking Pcgf3/5.** *A*, RNA-seq heat map of dysregulated expression transcripts with >2-fold expression differences in ES cells of the indicated genotypes. *Red*, high expression; *blue*, low expression. *B*, log2 expression values in Pcgf3$^{-/-}$ *versus* WT and Pcgf5$^{-/-}$ *versus* WT ES cells from expression RNA-seq. Probes were considered to be up-regulated (*red*) or down-regulated (*green*) if they had a log2 -fold change of >1. *C*, Venn diagram illustrating the overlap of up- and down-regulated genes in ES cells of the indicated genotypes. *D*, GO analysis of Pcgf3/5 target genes down-regulated after Pcgf3/5 double deletion based on −log10 (*p* value).

### *Pcgf3/5 positively regulate transcriptional activity in ES cells*

To probe the molecular mechanisms that underlie the differentiation phenotypes of Pcgf3/5-null ES cells, RNA extracted from Pcgf3$^{-/-}$, Pcgf5$^{-/-}$, Pcgf3$^{-/-}$/Pcgf5$^{-/-}$, and wild-type ES cells was subjected to RNA-seq. Total mRNA from two independent biological replicates of Pcgf3$^{-/-}$, Pcgf5$^{-/-}$, and Pcgf3$^{-/-}$/Pcgf5$^{-/-}$ cells were used for paired-end sequencing. As shown in Table S3, 318 differentially expressed genes were determined by comparing the Pcgf3 knockout and wild-type ES cells (102 up-regulated and 216 (68%) down-regulated genes), as determined by 2-fold cut-off, whereas 279 genes between the Pcgf5 knockout and wild-type ES cells were differentially expressed (80 up-regulated and 199 (71%) down-regulated genes) (Fig. 3, *A* and *B*). Notably, the Pcgf3$^{-/-}$ and Pcgf5$^{-/-}$ lists also exhibited significant overlap with each other (Fig. 3*C*). Analysis of the transcriptional profiling of Pcgf3/5 double mutant revealed a 30% increase in the number of genes significantly differentially expressed in the double mutant compared with the Pcgf3/5 single mutants (346 Pcgf3/5-dependent genes compared with 318 Pcgf3 or 279 Pcgf5-dependent genes) (Fig. 3*C*). Moreover, >70% of the genes significantly differentially expressed in the double mutant were down-regulated compared with wild type (Fig. 3*A* and Table S3). Based on gene ontology (GO) term analysis, there is no significant enrichment for specific functional categories or cellular processes within the Pcgf3/5-repressed genes. However, GO analysis of the down-regulated genes in Pcgf3$^{-/-}$ or Pcgf5$^{-/-}$, especially Pcgf3/5 double mutants, scored them as being statistically associated with mesoderm differentiation genes (*e.g.* cartilage development, blood vessel morphogenesis, and heart morphogenesis) (Fig. 3*D*), suggesting a particular role for Pcgf3/5 in mesoderm cell fate. Thus, these results strongly suggest that Pcgf3/5 predominantly act as transcriptional activators in ES cells. Overall, our data not only support the conclusion that Pcgf3 and Pcgf5 largely regulate the similar set of downstream genes, but also provide a molecular interpretation for the redundancy of Pcgf3 and Pcgf5 in ES cell differentiation.

### *Characterization of the PRC1.3 or PRC1.5 complex in ES cells*

Previous proteomic approaches identified Pcgf3 and Pcgf5 as components of non-canonical PRC1 complexes designated as PRC1.3 or PRC1.5, respectively, which contain Ring1B associated with Ck2, Rybp, and Auts2 in 293T-REx cells (12). To address the composition of PRC1.3 or PRC1.5 complexes in ES cells, we stably expressed a C-terminal FLAG-tagged form of Pcgf3 or Pcgf5 in Pcgf3$^{-/-}$ or Pcgf5$^{-/-}$ ES cells, respectively; affinity-purified it from nuclear extracts; and then used mass spectrometric analysis to determine associated proteins. MS analysis showed that Pcgf3/5 were strongly associated with core components of PRC1, including Ring1A/B, Rybp, and its homologue Yaf2, along with Wdr68, Fbrs, and casein kinase 2 (Ck2a1, Ck2a2, and Ck2b), which are unrelated to PRC1 (Fig. 4, *A* and *B*). As reported previously, Pcgf5 interacted with Auts2 in neurons and 293T-Rex cells (12, 16); however, we failed to detect any Auts2 from the Pcgf3/5 immunoprecipitates. As is consistent with previous studies, Pcgf3 and Pcgf5 were mutually exclusive, given that immunoprecipitation of Pcgf3 did not recover Pcgf5 and vice versa (Fig. 4, *B* and *C*).

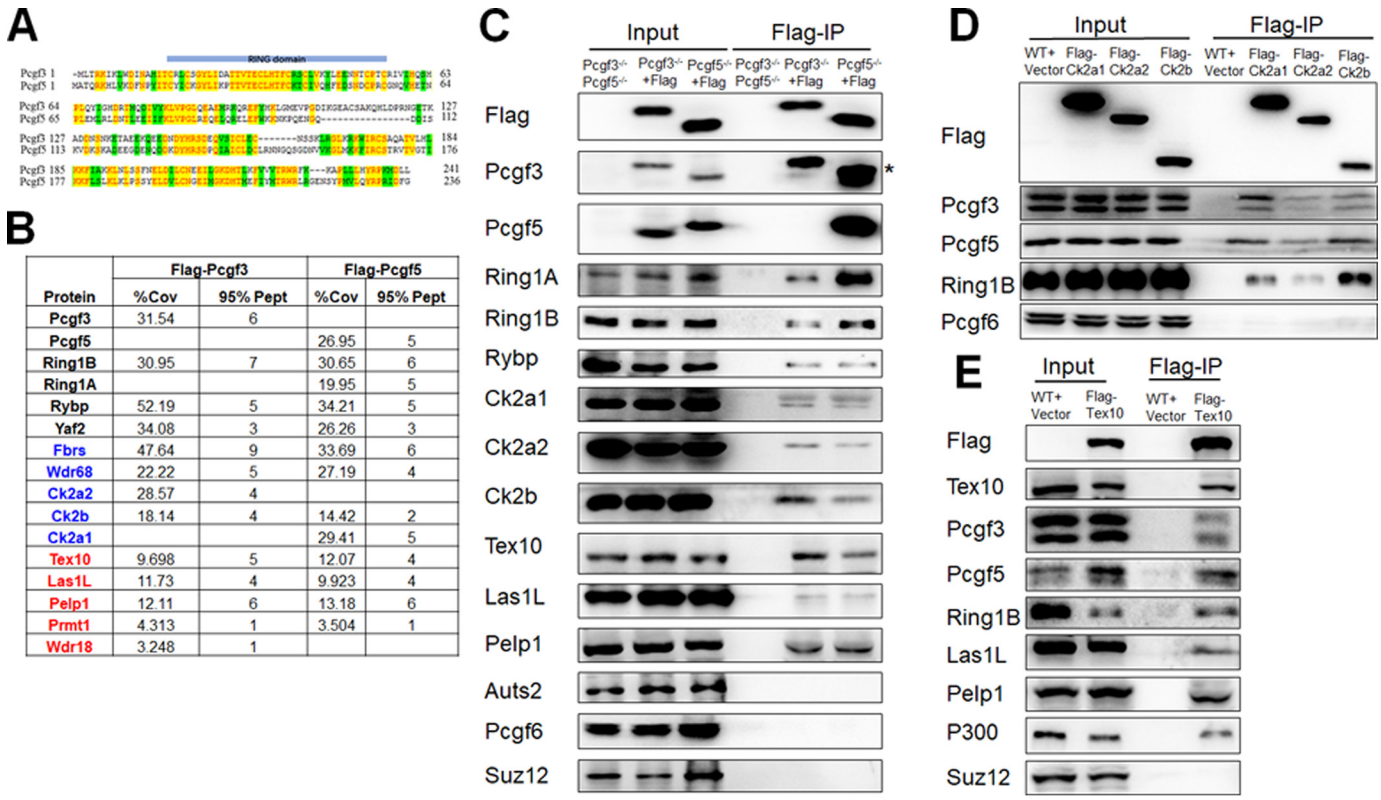


| Protein | Flag-Pcgf3 %Cov | Flag-Pcgf3 95% Pept | Flag-Pcgf5 %Cov | Flag-Pcgf5 95% Pept |
|---|---|---|---|---|
| Pcgf3 | 31.54 | 6 | | |
| Pcgf5 | | | 26.95 | 5 |
| Ring1B | 30.95 | 7 | 30.65 | 6 |
| Ring1A | | | 19.95 | 5 |
| Rybp | 52.19 | 5 | 34.21 | 5 |
| Yaf2 | 34.08 | 3 | 26.26 | 3 |
| Fbrs | 47.64 | 9 | 33.69 | 6 |
| Wdr68 | 22.22 | 5 | 27.19 | 4 |
| Ck2a2 | 28.57 | 4 | | |
| Ck2b | 18.14 | 4 | 14.42 | 2 |
| Ck2a1 | | | 29.41 | 5 |
| Tex10 | 9.698 | 5 | 12.07 | 4 |
| Las1L | 11.73 | 4 | 9.923 | 4 |
| Pelp1 | 12.11 | 6 | 13.18 | 6 |
| Prmt1 | 4.313 | 1 | 3.504 | 1 |
| Wdr18 | 3.248 | 1 | | |

**Figure 4. Characterization of the PRC1.3 and PRC1.5 complexes.** *A*, amino acid sequence alignment of full-length mouse Pcgf3 with mouse Pcgf5. The amino acid numbering for each sequence is indicated at the *right*. Identical and similar residues are indicated by *yellow* and *green*, respectively. *B*, list of Pcgf3- and Pcgf5-interacting proteins identified by MS. Protein complexes from nuclear lysates of Pcgf3$^{-/-}$ or Pcgf5$^{-/-}$ ES cells ectopically expressing FLAG-Pcgf3 or FLAG-Pcgf5, respectively, were recovered by MS. Proteins, 95% unique peptides (*95% Pept*), and percent coverage (% *Cov*) are indicated. PcG core proteins are in *black type*. The proteins that were identified by a previous study are *labeled* in *blue*. Proteins newly identified in this study are in *red type*. *C*, confirmation of Pcgf3- and Pcgf5-containing complexes by Immunoprecipitation-immunoblot analysis. Nuclear extracts from Pcgf3$^{-/-}$/Pcgf5$^{-/-}$ and Pcgf3$^{-/-}$/Pcgf5$^{-/-}$ ES cells rescued with FLAG-Pcgf3 (*Pcgf3*$^{-/-}$+*FLAG*) or FLAG-Pcgf5 (*Pcgf5*$^{-/-}$+*FLAG*), respectively, were subjected to immunoprecipitation using anti-FLAG M2-agarose beads. Bound proteins were separated on SDS-PAGE and detected by Western blotting with the indicated antibodies. Notably, the Pcgf3 antibody could nonspecifically bind Pcgf5 (*). *D*, immunoprecipitation from nuclear extract of ES cells expressing FLAG-Ck2a1, -Ck2a2, or -Ck2b using anti-FLAG M2 beads, followed by Western blotting with the antibodies indicated. *E*, immunoprecipitation from nuclear extract of ES cells expressing FLAG-Tex10 using anti-FLAG M2-agarose beads, followed by Western blotting with the antibodies indicated.

Next, immunoprecipitation experiments performed with nuclear extract of mutant ES cells reexpressing FLAG-tagged Pcgf3 or Pcgf5 and antibody against FLAG confirmed Pcgf3 or Pcgf5 association with Ring1A/B, Rybp, Ck2s, Tex10, Las1L, and Pelp1. As expected, other PcG components not associated with PRC1.3 or PRC1.5, such as Pcgf6 and Suz12, comprising PRC1.6 and PRC2, respectively, did not precipitate with Pcgf3 or Pcgf5 (Fig. 4*C*). To further confirm the interaction between Pcgf3/5 and Ck2s, we performed a reverse co-immunoprecipitation assay, with the results showing Pcgf3/5 but not Pcgf6 protein existing in the complex pulled down by the anti-FLAG antibody in wild-type ES cells stably expressing FLAG-tagged Ck2s (Ck2a1, Ck2a2, and Ck2b). Notably, our experiments showed that all Ck2 proteins (Ck2a1, Ck2a2, and Ck2b) interact with Pcgf3 and Pcgf5 by an immunoprecipitation assay (Fig. 4*D*), although some were missed in our mass spectrometric analysis (Fig. 4*B*). Most importantly, several proteins, including Tex10, Las1L, and Pelp1, were also recovered in Pcgf3 or Pcgf5 immunoprecipitates (Fig. 4*C*). Interestingly, Tex10, Las1L, and Pelp1 together with Senp3 and Wdr18 form a previously characterized complex referred to as five friends of methylated Chtop (5FMC) (23). Reciprocal immunoprecipitation was performed to verify the interaction between Pcgf3/5 and 5FMC complex in ES cells. Immunoprecipitation of FLAG-Tex10 in ES cells stably expressing FLAG-tagged Tex10 allowed the coprecipitation of Las1L, Pelp1, and Pcgf3/5, as evidenced by Western blotting analysis. Additionally, p300 was found in Tex10 precipitates (Fig. 4*E*), consistent with a previous study showing the interaction between Tex10 and p300 to control the histone acetylation (24). In summary, we have widened the set of multiunit Pcgf3/5 complexes in ES cells, and the new interactors, especially Tex10, Las1L, and Pelp1, might render these complexes capable of activating transcription not typically characterized as PcG functions.

### *Pcgf3 and Pcgf5 are essential for the recruitment of PRC1.3 or PRC1.5 complex to target genes*

As mentioned above, Pcgf3/5 predominantly activate transcription in ES cells, and mass spectrometric analysis further revealed that the Pcgf3/5 complex contains components involved in transcription activation. However, the contributions of these new components to Pcgf3/5-mediated transcription remain to be determined. To examine the local impact of Pcgf3/5 on chromatin features at promoters, we probed a panel of target genes enriched in mesodermal differentiation (Wisp1, Lhx9, Acta1, Sp5, Meis1, and Tgfb1), selected from genome-

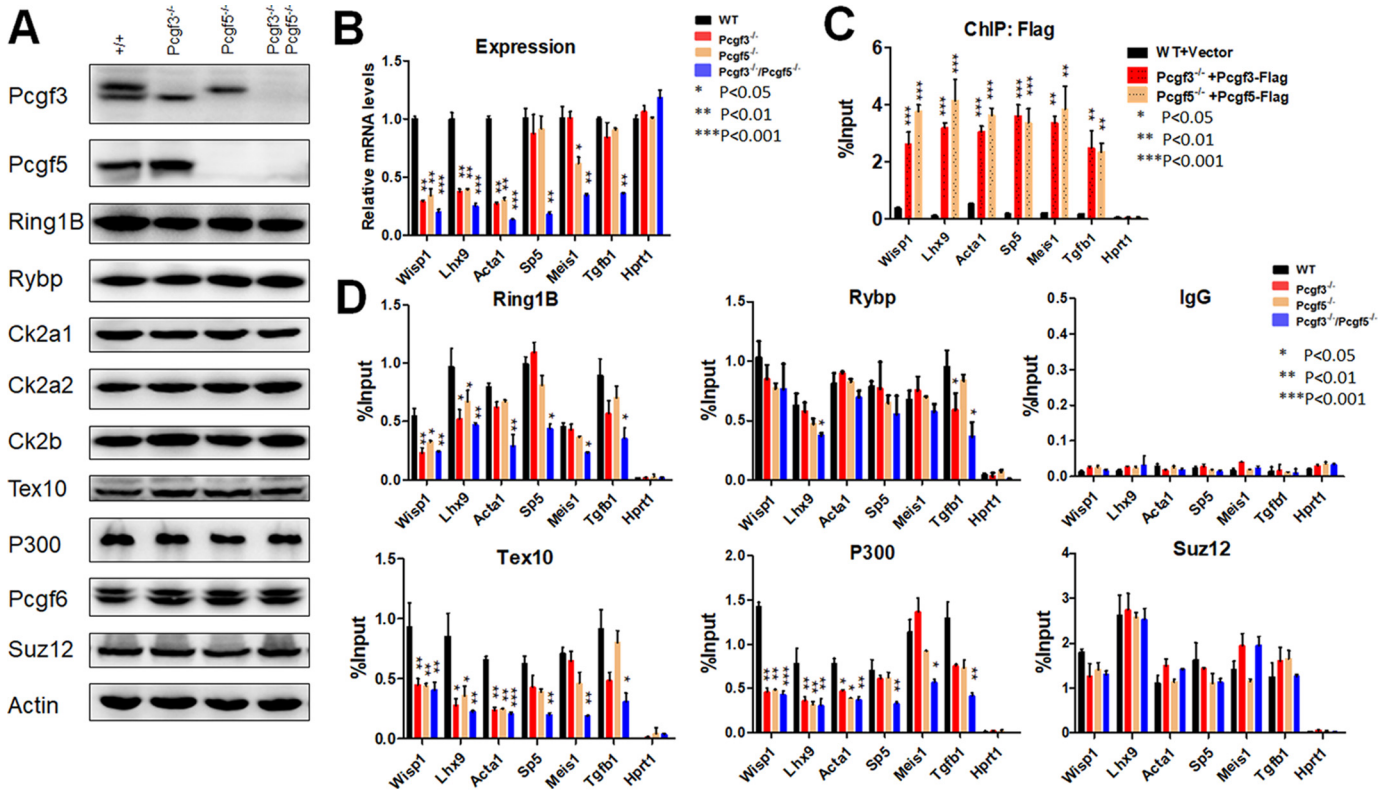


**Figure 5. Pcgf3/5 are essential for the recruitment of PRC1.3 or PRC1.5 complex to their target genes.** *A*, protein levels of PRC1.3 or PRC1.5 complex proteins, Suz12, and p300 were determined by Western blotting in ES cells of the indicated genotypes. *B*, expression analysis by RT-qPCR of RNA from ES cells of the indicated genotype for selected genes (Wisp1, Lhx9, Acta1, Sp5, Meis1, and Tgfb1). Hprt1 was used as a control. Expression was normalized to the housekeeping gene *β*-actin. *C*, ChIP of FLAG-Pcgf3 or FLAG-Pcgf5, followed by qPCR analysis. Direct target genes exhibited significantly higher signal in FLAG-Pcgf3– or FLAG-Pcgf5–rescued compared with mock-infected wild-type ES cells. *D*, ChIP-qPCR was used to analyze the occupancy of Ring1B, Rybp, Tex10, p300, Suz12, and IgG on the promoters of Pcgf3/5 targeting genes in ES cells. *Error bars*, S.D. Bar graphs represent the mean of three independent biological repeats. *p* values were from Student's *t* test analysis.

wide RNA-seq analysis, whose expression was down-regulated after Pcgf3/5 deletion. In particular, Wisp1 is involved in the migration and proliferation of vascular smooth muscle cells (25). Lhx9 is implicated in the correct development of many organs, including gonads, limbs, and heart (26–28). Acta1 is found in muscle tissues and is a major constituent of the contractile apparatus (29). Sp5 is dynamically expressed during development and genetically interacts with Brachyury (30). Meis1 is required for definitive hematopoiesis and vascular patterning (31). Tgfb1 is required for hematopoiesis and endothelial differentiation (32). Their differential expression and Pcgf3/5-binding status in undifferentiated and differentiating ES cells were verified by RT-qPCR and ChIP-qPCR analyses (Fig. 5 (*B* and *C*) and Fig. S6).

Next, we probed promoters of these Pcgf3/5 target genes for the presence of key components of PRC1.3 or PRC1.5 complex. Indeed, Ring1B, Rybp, and Tex10 were highly enriched at these target gene promoters (Fig. 5*D*), strongly suggesting that Pcgf3/5 and their associated PRC1 complexes target the developmental genes directly in ES cells. As Pcgf3/5 can physically associate with the PRC1.3/5 core components and also co-occupy the promoters of developmental genes in ES cells, it may contribute to the recruitment of these complexes to the promoters of these target genes. To investigate this possibility, we performed ChIP-qPCR analyses for Ring1B and Rybp under control and Pcgf3/5 single- or double-deleted conditions and compared their promoter occupancy. ChIP data indicated that recruitment of Ring1B was minimally or moderately affected by single or combined loss of Pcgf3/5, respectively (Fig. 5*D*). Consistent with the role of PRC1 in histone H2A ubiquitination, ChIP-qPCR analysis showed that the H2AK119ub1 levels at the target sites were also marginally or dramatically reduced in ES cells with Pcgf3/5, single or double knockout, respectively (see below). Of note, ChIP data indicated that recruitment of Rybp and Suz12 as well as H3K27me3 was generally not affected by loss of either protein individually or in combination (see below).

Most importantly, the deletion of both Pcgf3 and Pcgf5 also led to a strong reduction of Tex10 and transcriptional coactivator p300, a histone acetyltransferase, binding to target genes and, consistent with this, to a reduction in mRNA levels of the target genes (Fig. 5, *B* and *D*). In line with this, we found that deletion of Pcgf3/5 reduced enrichment of H3K27ac modifications on their targeting promoters (see below). As Pcgf3/5 disruption did not affect the global level of Ring1B, Tex10, or p300 (Fig. 5*A*), the most reasonable explanation for the decreased promoter occupancy of these components is that Pcgf3/5 contribute to their recruitment. These conclusions were further supported by analysis of the enrichment of Tex10, H3K27ac, and p300 on the promoters of Pcgf3/5 targeting genes in differentiating ES cells (Fig. S6). Taken together, the above results demonstrate that Pcgf3/5 are capable of mediating the recruitment of a PRC1.3 or PRC1.5 complex to developmental genes

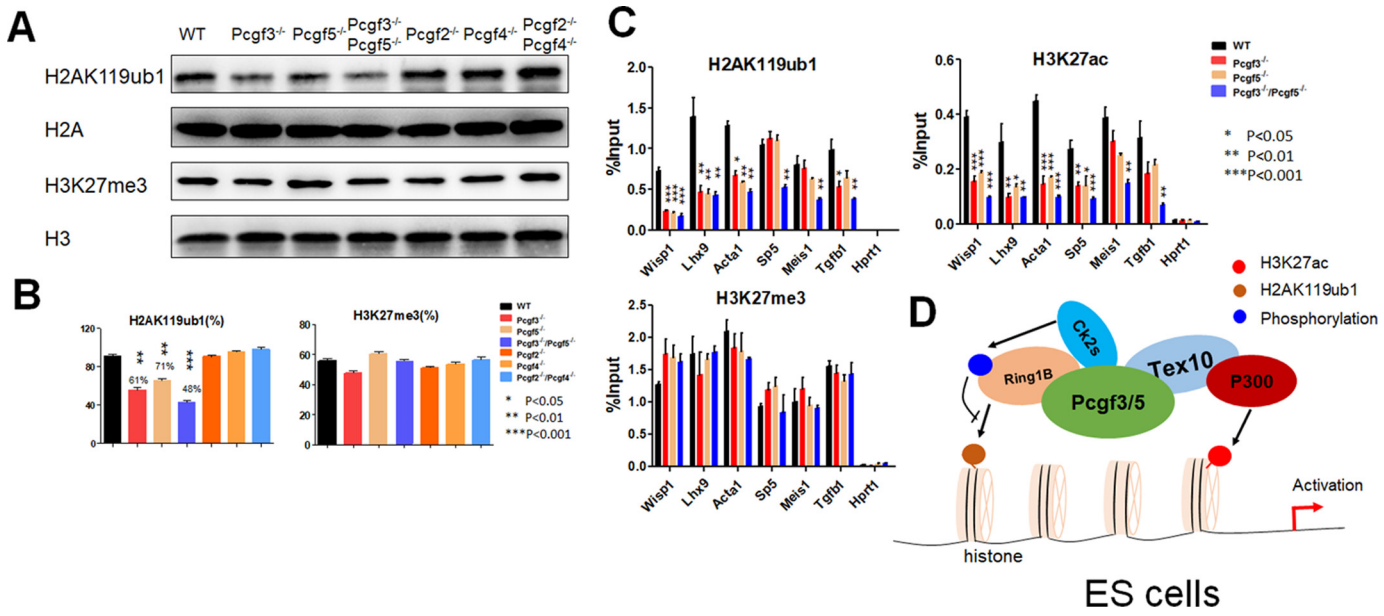


**Figure 6. Loss of Pcgf3/5 leads to substantially reduced levels of H2AK119ub1 in ES cells.** *A*, acid-extracted histones were prepared and analyzed by Western blot using the antibodies indicated. *B*, quantification of H2AK119ub1 and H3K27me3 levels was shown. Levels of H2AK119ub1 or H3K27me3 were normalized to the amount of H2A or H3, respectively. Bar graphs represent the mean of three independent biological repeats. *Error bars*, S.D. Data shown are representative of three separate experiments. *C*, ChIP showing the enrichment of H2AK119ub1, H3K27ac, and H3K27me3 on the target gene promoters in wild-type and mutant ES cells. *Error bars*, S.D. Bar graphs represent the mean of three independent biological repeats. *p* values are from Student's *t* test analysis. *D*, a model for Pcgf3/5-mediated transcriptional activation. See "Results section" for details.

to activate their expression in ES cells. These data also suggest that Pcgf3 and Pcgf5 share a substantial degree of functional redundancy in recruitment of the complex to chromatin, consistent with the exacerbated mesodermal defects observed in Pcgf3/5 double knockout EBs.

Tex10 has recently been reported to be critical in pluripotency and reprogramming via epigenetic regulation of superenhancer activity (24). To explore the possibility that Pcgf3/5 may cooperate with Tex10 in modulating the superenhancer activity, we examined the enrichment of Sox2, H3K27ac, Tex10, and Pcgf5 in the superenhancer regions of Oct4, Nanog, Sox2, and Esrrb loci. We found that these superenhancers are targeted by Sox2, H3K27ac, and Tex10, reinforcing the notion that Tex10 may contribute to ES cell-specific superenhancer activity (Fig. S7*A*). Pcgf5, however, was not detected in the regions of these selective superenhancers, suggesting that Pcgf3/5 may regulate ES cell functions in a superenhancer-independent manner. Supporting this, Sox2 was not detected at Pcgf3/5 target promoters, as evidenced by a ChIP assay (Fig. S7*B*). Intrigued by Tex10 and its physical interaction with Pcgf3/5, we sought to generate Tex10 knockout ES cell lines and compare them with Pcgf3/5-deficient cells. Homozygous Tex10 knockout ES cells generated by CRISPR/Cas9-mediated genome editing were unable to form compact colonies on feeder cells (Fig. S8). To circumvent the lethality associated with complete loss of this gene, we are generating ES cells with a conditionally targeted Tex10, which should allow us to test the functional cooperation between Pcgf3/5 and Tex10 in the future.

### *Loss of Pcgf3/5 leads to substantially reduced levels of H2AK119ub1 in ES cells*

PRC1 complexes share a common core heterodimer Ring1A/B and Pcgf1–6 with potential for monoubiquitination of histone H2A at lysine 119 (33). This raises the possibility that individual PCGF family members might confer differing H2AK119ub1 E3 ligase activities on PRC1. Although it has been reported that global H2AK119ub1 levels were significantly reduced in Ring1A/B double knockout ES cells (34), the role of PCGF in regulating H2A monoubiquitination remains to be examined. To determine whether PCGFs as non-catalytic components of PRC1 contribute to the H2AK119 ubiquitin E3 ligase activity, we isolated bulk histones from wild-type and PCGF mutant ES cells by acid extraction. As seen in Fig. 6 (*A* and *B*), the knockout of Pcgf3, Pcgf5, or both resulted in a 39, 29, and 52% decrease, respectively, in global levels of H2AK119ub1 as compared with wild-type cells, as evidenced by Western blotting. In contrast, no similar change was observed for H3K27me3. In addition, single or combined deletion of Pcgf2 and Pcgf4, components of canonical PRC1, unexpectedly did not exhibit a noticeable change in global H2AK119ub1 levels (Fig. 6, *A* and *B*). Considering the reduced H2AK119ub1 levels at the target sites in ES cells with loss of Pcgf3/5, it is likely that the local H2AK119ub1 reduction in Pcgf3/5$^{-/-}$ ES cells is probably also due to the reduction of global levels of H2AK119ub1 in addition to the decreased gene-specific Ring1B binding (Fig. 6*C*). Our observation is consistent with studies in cultured *Drosophila* cells, which show that L(3)73Ah, an orthologue of mammalian Pcgf3, contributes widely to H2AK118ub1 (17). Also consistent with a function of Pcgf3/5 in the establishment of H2AK119ub1, Pcgf5-deficient hematopoietic stem and progenitor cells display a significant reduction in H2AK119ub1 levels compared with the control (35). Together with our previous finding that Pcgf1 and Pcgf6 are dispensable for the maintenance of H2AK119ub1 in ES cells (19, 20), these results suggest that of the PCGF family members,

only Pcgf3/5 are important for PRC1-mediated deposition of H2AK119ub1 in ES cells.

## Discussion

PRC1 proteins are well-known to be associated with transcriptional repression through epigenetic mechanisms, including histone modification H2AK119ub1 and chromatin compaction (36, 37). Genetic evidence suggests that the canonical PRC1 (PRC1.2 and PRC1.4) is required for transcriptional repression (7). A canonical PRC1 complex contains one of five different Cbx protein subunits (Cbx2/4/6/7/8) that specifically interact with H3K27me3 via its chromodomain and enable PRC1 recruitment to its target loci (38). Despite the recent advances made in understanding the role of PcG complexes in the epigenetic regulation of gene repression involved in various developmental processes (7, 39), how some of these complexes may interact with the general transcription machinery to contribute to the transcriptional activation remains elusive. In this study, we found that, in contrast to the canonical role of PRC1 in gene repression, Pcgf3/5 predominantly act as transcriptional activators driving expression of a number of genes involved in mesoderm differentiation. To obtain a better understanding of the role of Pcgf3/5 in transcriptional control of differentiation, we took a combined approach of immunoprecipitation followed by MS to shed light on the Pcgf3/5 interactome in ES cells (Fig. 4, *B* and *C*). Besides known Pcgf3/5-binding proteins, we also identified a set of additional proteins, of which three (Tex10, Las1L, and Pelp1) were of particular interest, due to the fact that they are often co-purified together as a part of the 5FMC (five friends of methylated Chtop) (23), Rix (40), Sox2 (24), and MLL1/MLL (41) complexes, which play such essential roles as linking arginine methylation to desumoylation for transcriptional activation, regulating ribosome biogenesis, establishing the ground state of pluripotency in ES cells, and modulating H3K4 methylation levels, respectively. Additionally, PRC1.5 has also been reported to turn on gene expression through recruiting Ck2 and co-activator p300 by one of its core components, Auts2, in developing neuronal cells (16). However, Auts2 was not detected in Pcgf3/5 precipitates in ES cells in the presence of overall normal expression levels of Auts2, suggesting that the natural variation in the composition of PRC1 complexes can engender PRC1 taking on unanticipated roles in coordinating cell type– and developmental stage–specific gene expression profiles. Overall, detailed mechanisms by which Pcgf3/5 control transcription in ES cells still remain unclear, and further investigations are needed to determine the influence of specific associated factors, especially the 5FMC members Tex10, Las1L, and Pelp1, on the activities of PRC1.3/5 complexes and their impact on PRC1-mediated transcriptional activation.

Pcgf3 and Pcgf5 as well as Pcgf1 have been demonstrated to contribute to H2AK119ub1-dependent recruitment of PRC2 and H3K27me3 modification in a *de novo* targeting assay in mouse ES cells (42). Therefore, we expected to see decreased levels of H3K27me3 at the Pcgf3/5 target genes in ES cells with single or combined deletion of Pcgf3 and Pcgf5. However, although reduction in the levels of H2AK119ub1 at the Pcgf3/5-selected promoters was detected in these mutants, no significant H3K27me3 change was observed. The molecular mechanism underlying this epigenomic alteration remains to be investigated in the future. Additionally, in ES cells with Pcgf3/5 single or combined loss, we identified moderately or drastically reduced, respectively, global and local levels of H2AK119ub1. It is worth bearing in mind that the E3 enzymatic activity of Ring1B is not essential for early mouse development and for global target gene (43) or Hox loci repression (44) in mouse ES cells and in *Drosophila* embryos (45), which raises questions about the precise role of this posttranslational modification in transcriptional regulation and argues for a re-evaluation of this H2AK119ub1-PRC1 functional paradigm. Ongoing studies are aimed at understanding how this epigenomic alteration contributes to Pcgf3/5-mediated transcriptional activation during ES cell differentiation.

## Experimental procedures

### *Construction of sgRNA-expressing plasmids and lentiviral expression vectors*

The sgRNA expression plasmid (pX330, Addgene plasmid ID 42230) was used to generate targeting gene deletion in ES cells. To minimize off-targeting effects, the sgRNAs were designed by the CRISPR design tool (18). The 20 oligonucleotide sequences that come before a 5′-NGG PAM sequence were selected to induce DNA double-strand breaks. A pair of annealed oligonucleotides was ligated into the BbsI-linearized sgRNA scaffold of pX330 vector. The sgRNA expression plasmids were verified by sequencing. To generate lentiviral expression vectors, the full-length cDNA for Pcgf3 (Q8BTQ0) and Pcgf5 (Q3UK78) was modified by integrating the sequence for a C-terminal FLAG tag (DYKDDDDK) into the reverse PCR primer, followed by cloning into pBluescript KS II. The resulting products were subcloned (NotI-BamHI) into lentiviral vector (46). The complete coding sequence of all expression vectors was verified by sequencing.

### *Generation of mutant ES cells*

The pair of sgRNA-expressing constructs were co-transfected with a plasmid encoding puromycin resistance into ES cells (B6 JN). 24 h after transfection, ES cells were selected by puromycin (2 $\mu$g/ml) for 48 h and then seeded on mitomycin-irradiated mouse embryonic fibroblasts on gelatinized tissue culture plates in DMEM supplemented with 15% ES cell fetal calf serum (ThermoFisher), LIF, non-essential amino acids (ThermoFisher), L-glutamine (ThermoFisher), 0.1 mM $\beta$-mercaptoethanol, and penicillin/streptomycin (ThermoFisher) as described (19). Correctly targeted knockout ES cell clones were identified by genomic PCR analysis. Subsequently, the absence of the protein in established null ES cells is confirmed by Western blotting analysis.

### *Lentiviral supernatant production and infection*

Lentiviral supernatants were prepared as described (46). The ES cells were infected with lentiviral supernatants in the presence of Polybrene (Sigma; final concentration of 8 $\mu$g/ml). After 24 h, the puromycin was used to screen positive ES cells.

### *Embryoid body formation and analysis*

Embryoid body formation was performed using the hanging drop assay as described (46). First, ES cells were trypsinized and resuspended in Iscove's modified Dulbecco's medium without LIF (2 mM L-glutamine, penicillin/streptomycin, non-essential amino acids, 50 $\mu$g/ml ascorbic, 200 $\mu$g/ml iron-saturated holotransferrin, sodium pyruvate, 450 $\mu$M monothioglycerol, and 15% ES cell fetal calf serum). 30 $\mu$l (about 300 cells) was pipetted onto a Petri dish plate lid. Hanging drops were cultured for 3 days (37 °C, 5% $CO_2$). After 3 days, EBs were collected and cultured on a rotating shaker. The images of EB morphology were taken by the Olympus system. Total RNA was collected at days 3, 7, and 12 and analyzed by RT-qPCR.

### *Affinity purification, immunoprecipitation, and mass spectrometry*

Pcgf3$^{-/-}$ or Pcgf5$^{-/-}$ ES cells rescued with Pcgf3-FLAG or Pcgf5-FLAG, respectively, were used for the affinity purification experiment. Cell pellet was suspended in 5 ml of hypotonic lysis buffer (10 mM Tris-Cl, pH 8.0, 1 mM KCl, 1.5 mM $MgCl_2$, 1 mM DTT, 0.2 mM PMSF, 10 mM $Na_4P_2O_7$, 2 mM $Na_3VO_4$, 100 mM NaF, protease inhibitor mix (Sigma)) and incubated for 30 min on a rotator at 4 °C. The suspension was then subjected to 10,000 × *g* centrifugation at 4 °C for 10 min. The resulting nuclear pellet was resuspended in 2 ml of nuclear lysis buffer (20 mM Tris-HCl, pH 8.0, 25% glycerol, 420 mM NaCl, 1.5 mM $MgCl_2$, 0.2 mM EDTA, 0.5 mM DTT, 1% Triton X-100, protease inhibitors). After rotation at 4 °C for 30 min, the suspension was centrifuged at 12,000 × *g* at 4 °C for 30 min, and the supernatant was nuclear extract. For immunoprecipitation, 1.5 ml of nuclear extract was mixed with 3 ml of hypotonic lysis buffer and 100 $\mu$l of prewashed M2 beads (A2220, Sigma). After rotation at 4 °C overnight, the M2 beads were spun down at 2000 × *g* at 4 °C for 2 min. The beads were washed with wash buffer (two-thirds volume of hypotonic lysis buffer, one-third volume of nuclear lysis buffer) four times and then eluted with 50 $\mu$l of FLAG peptides at 1 mg/ml in wash buffer by rotating at 4 °C for 1 h three times. The eluates were resolved on SDS-PAGE, followed by Western blotting. For MS identification, the eluates were run into the SDS-polyacrylamide gel about 1 cm, stained by Coomassie Blue. The gel slice containing all proteins was cut and sent for liquid chromatography MS analysis (2D-NanoLC/TripleTOF5600).

### *Whole-cell lysates, histone extraction, and Western blotting analysis*

ES cells were resuspended in radioimmune precipitation assay buffer (50 mM Tris-HCl, pH 8.0, 150 mM NaCl, 1% Triton X-100, 0.5% sodium deoxycholate, 0.1% SDS, 1 mM EDTA, 2 mM $Na_3VO_4$, 100 mM NaF, 1 mM DTT, 10 mg/ml PMSF, and protease inhibitor mix (Sigma)). Lysates were incubated for 30 min on ice and precleared by centrifugation at 12,000 rpm at 4 °C for 30 min. Proteins were separated by SDS-PAGE and analyzed by immunoblotting. Histone extraction was performed as described (47). Briefly, ES cells were resuspended in 1 ml of hypotonic lysis buffer and incubated for 30 min on a rotator at 4 °C. The intact nuclei were spun in a cooled tabletop centrifuge at 10,000 × *g* for 10 min at 4 °C. The nuclear pellet was resuspended in 200 $\mu$l of 0.2 N HCl. Histone modifications were analyzed by Western blotting. A list of the antibodies used in this study is shown in Table S1.

### *Expression analysis*

Total RNA was harvested from ES cells or EBs using TRIzol (ThermoFisher). RT was carried out with 2 $\mu$g of total RNA using oligo(dT), random hexamers, and Moloney murine leukemia virus reverse transcriptase (Invitrogen). Real-time PCR was performed using PowerUp™ SYBR® Green Master Mix (Invitrogen) on StepOne™ software version 2.3 (Applied Biosystems). The mRNA level was normalized to $\beta$-actin. Primers for real-time qPCR are shown in Table S2.

### *RNA-seq*

RNA was prepared using the TRIzol reagent (ThermoFisher), following the manufacturer's recommendations. RNA was quantified using a NanoDrop-1000 spectrophotometer. Sequencing libraries were generated using the NEBNext® Ultra™ RNA Library Prep Kit for Illumina® (catalog no. E7530L, New England Biolabs) and then were sequenced on an Illumina Hiseq4000 platform and generated 150-bp paired-end reads. The sequencing data were mapped against the mm10 mouse genome assembly using TopHat version 2.0.12 (48). The read counts of genes were counted by HTSeq version 0.6.0, and the expression levels of genes were calculated by FPKM (fragments per kilobase of transcript per million fragments mapped) (49). Next, differential gene expression analysis between wild-type and mutant ES cells was estimated by DESeq (version 1.16) (50). Lists of up- and down-regulated genes in mutant as compared with wild-type samples are shown in Table S3. In addition, RNA-seq data were deposited at the Gene Expression Omnibus under accession number GSE102774.

### *Teratoma formation and analysis*

The experimental animal facility has been accredited by the Association for Assessment and Accreditation of Laboratory Animal Care International, and the institutional animal care and use committee of the Model Animal Research Center of Nanjing University approved all animal protocols used in this study. Teratoma formation was performed as described previously (46). Briefly, 1 × $10^6$ ES cells were injected subcutaneously into the flanks of nude mice. After 3 weeks, teratomas were excised and fixed in 4% phosphate-buffered formaldehyde overnight at 4 °C. Paraffin-embedded tissue was sliced and stained with hematoxylin and eosin. Immunohistochemistry was performed by using antibodies listed in Table S1.

### *ChIP*

ChIP analysis was performed as described (46). ES cells were cross-linked by the addition of fresh formaldehyde solution (37%) to a final concentration of 1% for 10 min at room temperature on a rotator. The reaction was quenched by adding glycine to a final concentration of 0.125 M. Cells were washed three times with ice-cold PBS and subjected to 2,000 × *g* centrifugation at 4 °C for 5 min. Cells were lysed in ChIP buffer (50 mM Tris, pH 8.0, 10 mM EDTA, 1% SDS, protease inhibitors) for 20 min on ice, and subsequently chromatin DNA was sheared into

small fragments (200–1000 bp) by the Bioruptor system (Diagenode). For immunoprecipitation, 1 volume of chromatin solution was mixed with 4 volumes of ChIP dilution buffer (0.01% SDS, 1.1% Triton X-100, 1.1 mM EDTA, 20 mM Tris-Cl, pH 8.0, 167 mM NaCl, protease inhibitors) and appropriate antibodies. Rabbit or mouse IgG was used as control. After rotation at 4 °C for 2 h, immunocomplexes were captured with protein A/G-Sepharose overnight at 4 °C. The beads were washed twice with low-salt buffer (150 mM NaCl, 20 mM Tris, pH 8.0, 1 mM EDTA, 0.1% SDS, 1% Triton X-100, 0.5% sodium deoxycholate, protease inhibitors) and then washed with high-salt buffer twice. Immunocomplexes were eluted by eluent buffer (1% SDS, 100 mM $NaHCO_3$) at 65 °C. DNA cross-linking was reversed by adding NaCl to a final concentration of 0.2 M at 65 °C overnight, and then DNA was purified using a DNA gel extraction kit (Axygen). To prepare an input control, whole-cell extract DNA (reserved from the sonication step) was also treated by reverse cross-linking. Quantitative PCRs were performed using PowerUp™ SYBR® Green Master Mix (ThermoFisher) on StepOne™ software version 2.3 (Applied Biosystems). The enrichment was calculated as $2^{-\Delta Ct}$, where $\Delta Ct = Ct(\text{ChIP}) - Ct(\text{input})$. Primers utilized for ChIP are listed in Table S2.

*Author contributions*—W. Z. performed RT-qPCR, ChIP-qPCR, and Western blot analysis; carried out the LC-MS analysis with the help of J. Z. and C. L.; and analyzed all experiments. Y. H. genotyped and characterized Pcgf3/5 knockout ES cells with the help of W. Z. and M. L. H. J. performed the immunohistochemistry with the help of C. W. and N. C. Y. X. provided advice on experimental design and collected and organized data, with the assistance of Q. J. J. Q. designed, analyzed, and supervised the research and wrote the manuscript with the help of W. Z. The manuscript was critically reviewed and approved by all authors.

*Acknowledgments—We thank Drs. Zhaoyu Lin and Xiang Gao for providing lentivirus expression vector. We are indebted to Drs. Lei Fang and Bin Xue for kindly providing reagents and technical advice.*

*Addendum*—While this manuscript was in preparation, we became aware of an interesting study done by Almeida *et al.* (51). This study, which was done independently, provides *in vivo* support for our *in vitro* findings that Pcgf3/5 play an essential role in ES cell pluripotency and early embryonic development.

## References


1. Nishikawa, S., Jakt, L. M., and Era, T. (2007) Embryonic stem-cell culture as a tool for developmental cell biology. *Nat. Rev. Mol. Cell Biol.* **8,** 502–507
2. Evans, M. (2011) Discovering pluripotency: 30 years of mouse embryonic stem cells. *Nat. Rev. Mol. Cell Biol.* **12,** 680–686
3. Morey, L., Santanach, A., and Di Croce, L. (2015) Pluripotency and epigenetic factors in mouse embryonic stem cell fate regulation. *Mol. Cell. Biol.* **35,** 2716–2728
4. Aloia, L., Di Stefano, B., and Di Croce, L. (2013) Polycomb complexes in stem cells and embryonic development. *Development* **140,** 2525–2534
5. Lewis, E. B. (1978) A gene complex controlling segmentation in *Drosophila*. *Nature* **276,** 565–570
6. Simon, J. A., and Kingston, R. E. (2009) Mechanisms of polycomb gene silencing: knowns and unknowns. *Nat. Rev. Mol. Cell Biol.* **10,** 697–708
7. Aranda, S., Mas, G., and Di Croce, L. (2015) Regulation of gene transcription by Polycomb proteins. *Sci. Adv.* **1,** e1500737
8. Margueron, R., and Reinberg, D. (2011) The Polycomb complex PRC2 and its mark in life. *Nature* **469,** 343–349
9. Cao, R., Wang, L., Wang, H., Xia, L., Erdjument-Bromage, H., Tempst, P., Jones, R. S., and Zhang, Y. (2002) Role of histone H3 lysine 27 methylation in Polycomb-group silencing. *Science* **298,** 1039–1043
10. Wang, H., Wang, L., Erdjument-Bromage, H., Vidal, M., Tempst, P., Jones, R. S., and Zhang, Y. (2004) Role of histone H2A ubiquitination in Polycomb silencing. *Nature* **431,** 873–878
11. Gil, J., and O'Loghlen, A. (2014) PRC1 complex diversity: where is it taking us? *Trends Cell Biol.* **24,** 632–641
12. Gao, Z., Zhang, J., Bonasio, R., Strino, F., Sawai, A., Parisi, F., Kluger, Y., and Reinberg, D. (2012) PCGF homologs, CBX proteins, and RYBP define functionally distinct PRC1 family complexes. *Mol. Cell* **45,** 344–356
13. Creppe, C., Palau, A., Malinverni, R., Valero, V., and Buschbeck, M. (2014) A Cbx8-containing Polycomb complex facilitates the transition to gene activation during ES cell differentiation. *PLoS Genet.* **10,** e1004851
14. Frangini, A., Sjöberg, M., Roman-Trufero, M., Dharmalingam, G., Haberle, V., Bartke, T., Lenhard, B., Malumbres, M., Vidal, M., and Dillon, N. (2013) The aurora B kinase and the polycomb protein ring1B combine to regulate active promoters in quiescent lymphocytes. *Mol. Cell* **51,** 647–661
15. Kondo, T., Isono, K., Kondo, K., Endo, T. A., Itohara, S., Vidal, M., and Koseki, H. (2014) Polycomb potentiates meis2 activation in midbrain by mediating interaction of the promoter with a tissue-specific enhancer. *Dev. Cell* **28,** 94–101
16. Gao, Z., Lee, P., Stafford, J. M., von Schimmelmann, M., Schaefer, A., and Reinberg, D. (2014) An AUTS2-Polycomb complex activates gene expression in the CNS. *Nature* **516,** 349–354
17. Lee, H.-G., Kahn, T. G., Simcox, A., Schwartz, Y. B., and Pirrotta, V. (2015) Genome-wide activities of Polycomb complexes control pervasive transcription. *Genome Res.* **25,** 1170–1181
18. Ran, F. A., Hsu, P. D., Wright, J., Agarwala, V., Scott, D. A., and Zhang, F. (2013) Genome engineering using the CRISPR-Cas9 system. *Nat. Protoc.* **8,** 2281–2308
19. Zhao, W., Tong, H., Huang, Y., Yan, Y., Teng, H., Xia, Y., Jiang, Q., and Qin, J. (2017) Essential role for Polycomb group protein Pcgf6 in embryonic stem cell maintenance and a noncanonical polycomb repressive complex 1 (PRC1) integrity. *J. Biol. Chem.* **292,** 2773–2784
20. Yan, Y., Zhao, W., Huang, Y., Tong, H., Xia, Y., Jiang, Q., and Qin, J. (2017) Loss of Polycomb group protein Pcgf1 severely compromises proper differentiation of embryonic stem cells. *Sci. Rep.* **7,** 46276
21. Evans, M. J., and Kaufman, M. H. (1981) Establishment in culture of pluripotential cells from mouse embryos. *Nature* **292,** 154–156
22. Morey, L., Santanach, A., Blanco, E., Aloia, L., Nora, E. P., Bruneau, B. G., and Di Croce, L. (2015) Polycomb regulates mesoderm cell fate-specification in embryonic stem cells through activation and repression mechanisms. *Cell Stem Cell* **17,** 300–315
23. Fanis, P., Gillemans, N., Aghajanirefah, A., Pourfarzad, F., Demmers, J., Esteghamat, F., Vadlamudi, R. K., Grosveld, F., Philipsen, S., and van Dijk, T. B. (2012) Five friends of methylated chromatin target of protein-arginine-methyltransferase [prmt]-1 (chtop), a complex linking arginine methylation to desumoylation. *Mol. Cell. Proteomics* **11,** 1263–1273
24. Ding, J., Huang, X., Shao, N., Zhou, H., Lee, D.-F., Faiola, F., Fidalgo, M., Guallar, D., Saunders, A., Shliaha, P. V., Wang, H., Waghray, A., Papatsenko, D., Sánchez-Priego, C., Li, D., *et al.* (2015) Tex10 coordinates epigenetic control of super-enhancer activity in pluripotency and reprogramming. *Cell Stem Cell* **16,** 653–668
25. Liu, H., Dong, W., Lin, Z., Lu, J., Wan, H., Zhou, Z., and Liu, Z. (2013) CCN4 regulates vascular smooth muscle cell migration and proliferation. *Mol. Cells* **36,** 112–118
26. Yang, Y., and Wilson, M. J. (2015) Lhx9 gene expression during early limb development in mice requires the FGF signalling pathway. *Gene Expr. Patterns* **19,** 45–51
27. Birk, O. S., Casiano, D. E., Wassif, C. A., Cogliati, T., Zhao, L., Zhao, Y., Grinberg, A., Huang, S., Kreidberg, J. A., Parker, K. L., Porter, F. D., and Westphal, H. (2000) The LIM homeobox gene Lhx9 is essential for mouse gonad formation. *Nature* **403,** 909–913

28. Smagulova, F. O., Manuylov, N. L., Leach, L. L., and Tevosian, S. G. (2008) GATA4/FOG2 transcriptional complex regulates Lhx9 gene expression in murine heart development. *BMC Dev. Biol.* **8,** 67
29. Gunning, P. W., Ferguson, V., Brennan, K. J., and Hardeman, E. C. (2001) α-skeletal actin induces a subset of muscle genes independently of muscle differentiation and withdrawal from the cell cycle. *J. Cell Sci.* **114,** 513–524
30. Harrison, S. M., Houzelstein, D., Dunwoodie, S. L., and Beddington, R. S. (2000) Sp5, a new member of the Sp1 family, is dynamically expressed during development and genetically interacts with Brachyury. *Dev. Biol.* **227,** 358–372
31. Azcoitia, V., Aracil, M., Martínez-A, C., Torres, M. (2005) The homeodomain protein Meis1 is essential for definitive hematopoiesis and vascular patterning in the mouse embryo. *Dev. Biol.* **280,** 307–320
32. Dickson, M. C., Martin, J. S., Cousins, F. M., Kulkarni, A. B., Karlsson, S., and Akhurst, R. J. (1995) Defective haematopoiesis and vasculogenesis in transforming growth factor-β1 knock out mice. *Development* **121,** 1845–1854
33. McGinty, R. K., Henrici, R. C., and Tan, S. (2014) Crystal structure of the PRC1 ubiquitylation module bound to the nucleosome. *Nature* **514,** 591–596
34. Endoh, M., Endo, T. A., Endoh, T., Isono, K., Sharif, J., Ohara, O., Toyoda, T., Ito, T., Eskeland, R., Bickmore, W. A., Vidal, M., Bernstein, B. E., and Koseki, H. (2012) Histone H2A mono-ubiquitination is a crucial step to mediate PRC1-dependent repression of developmental genes to maintain ES cell identity. *PLoS Genet.* **8,** e1002774
35. Si, S., Nakajima-Takagi, Y., Aoyama, K., Oshima, M., Saraya, A., Sugishita, H., Nakayama, M., Ishikura, T., Koseki, H., and Iwama, A. (2016) Loss of Pcgf5 affects global H2A monoubiquitination but not the function of hematopoietic stem and progenitor cells. *PLoS One* **11,** e0154561
36. Eskeland, R., Freyer, E., Leeb, M., Wutz, A., and Bickmore, W. (2010) Histone acetylation and the maintenance of chromatin compaction by Polycomb repressive complexes. *Cold Spring Harbor Symp. Quant. Biol.* **75,** 71–78
37. Di Croce, L., and Helin, K. (2013) Transcriptional regulation by Polycomb group proteins. *Nat. Struct. Mol. Biol.* **20,** 1147–1155
38. Luis, N. M., Morey, L., Di Croce, L., and Benitah, S. A. (2012) Polycomb in stem cells: PRC1 branches out. *Cell Stem Cell* **11,** 16–21
39. Kondo, T., Ito, S., and Koseki, H. (2016) Polycomb in transcriptional phase transition of developmental genes. *Trends Biochem. Sci.* **41,** 9–19
40. Castle, C. D., Cassimere, E. K., and Denicourt, C. (2012) LAS1L interacts with the mammalian Rix1 complex to regulate ribosome biogenesis. *Mol. Biol. Cell* **23,** 716–728
41. Dou, Y., Milne, T. A., Tackett, A. J., Smith, E. R., Fukuda, A., Wysocka, J., Allis, C. D., Chait, B. T., Hess, J. L., and Roeder, R. G. (2005) Physical association and coordinate function of the H3 K4 methyltransferase MLL1 and the H4 K16 acetyltransferase MOF. *Cell* **121,** 873–885
42. Blackledge, N. P., Farcas, A. M., Kondo, T., King, H. W., McGouran, J. F., Hanssen, L. L., Ito, S., Cooper, S., Kondo, K., Koseki, Y., Ishikura, T., Long, H. K., Sheahan, T. W., Brockdorff, N., Kessler, B. M., *et al.* (2014) Variant PRC1 complex-dependent H2A ubiquitylation drives PRC2 recruitment and polycomb domain formation. *Cell* **157,** 1445–1459
43. Illingworth, R. S., Moffat, M., Mann, A. R., Read, D., Hunter, C. J., Pradeepa, M. M., Adams, I. R., and Bickmore, W. A. (2015) The E3 ubiquitin ligase activity of RING1B is not essential for early mouse development. *Genes Dev.* **29,** 1897–1902
44. Endoh, M., Endo, T. A., Endoh, T., Isono, K., Sharif, J., Ohara, O., Toyoda, T., Ito, T., Eskeland, R., Bickmore, W. A., Vidal, M., Bernstein, B. E., and Koseki, H. (2012) Histone H2A mono-ubiquitination is a crucial step to mediate PRC1-dependent repression of developmental genes to maintain ES cell identity. *PLoS Genet.* **8,** e1002774
45. Pengelly, A. R., Kalb, R., Finkl, K., and Müller, J. (2015) Transcriptional repression by PRC1 in the absence of H2A monoubiquitylation. *Genes Dev.* **29,** 1487–1492
46. Qin, J., Whyte, W. A., Anderssen, E., Apostolou, E., Chen, H. H., Akbarian, S., Bronson, R. T., Hochedlinger, K., Ramaswamy, S., Young, R. A., and Hock, H. (2012) The polycomb group protein L3mbtl2 assembles an atypical PRC1-family complex that is essential in pluripotent stem cells and early development. *Cell Stem Cell* **11,** 319–332
47. Shechter, D., Dormann, H. L., Allis, C. D., and Hake, S. B. (2007) Extraction, purification and analysis of histones. *Nat. Protoc.* **2,** 1445–1457
48. Kim, D., Pertea, G., Trapnell, C., Pimentel, H., Kelley, R., and Salzberg, S. L. (2013) TopHat2: accurate alignment of transcriptomes in the presence of insertions, deletions and gene fusions. *Genome Biol.* **14,** R36
49. Ojesina, A. I., Lichtenstein, L., Freeman, S. S., Pedamallu, C. S., Imaz-Rosshandler, I., Pugh, T. J., Cherniack, A. D., Ambrogio, L., Cibulskis, K., Bertelsen, B., Romero-Cordoba, S., Treviño, V., Vazquez-Santillan, K., Guadarrama, A. S., Wright, A. A., *et al.* (2014) Landscape of genomic alterations in cervical carcinomas. *Nature* **506,** 371–375
50. Trapnell, C., Roberts, A., Goff, L., Pertea, G., Kim, D., Kelley, D. R., Pimentel, H., Salzberg, S. L., Rinn, J. L., and Pachter, L. (2012) Differential gene and transcript expression analysis of RNA-seq experiments with TopHat and Cufflinks. *Nat. Protoc.* **7,** 562–578
51. Almeida, M., Pintacuda, G., Masui, O., Koseki, Y., Gdula, M., Cerase, A., Brown, D., Mould, A., Innocent, C., Nakayama, M., Schermelleh, L., Nesterova, T. B., Koseki, H., and Brockdorff, N. (2017) PCGF3/5–PRC1 initiates Polycomb recruitment in X chromosome inactivation. *Science* **356,** 1081–1084